$\Delta S^*/R$ values are respectively 12700 (±0.96%) and −135.99 (±0.07%) for the nonspectral data (77 observations) and 12912 (±0.68%) and −135.49 (±0.14%) for the spectral data (49 values based on the new molar absorptivity equations at 360 nm). At 425, 500, and 575 K, the vapor pressures based on the nonspectral data are $(3.2 \pm 0.6) \times 10^{-5}$, $(9.9 \pm 1.5) \times 10^{-3}$, and 0.60 ± 0.07 atm, respectively. The corresponding pressures based on the spectral data with the new molar absorptivities are 3.2×10^{-5}, 1.1×10^{-2}, and 0.68 atm and with the previous molar absorptivities are 3.6×10^{-5}, 1.2×10^{-2}, and 0.76 atm. The match between the nonspectral and the spectral vapor pressures is now more reasonable with the new molar absorptivities. A least-squares treatment of the combined data (126 total observations) gives the recommended constants, 12613 (±0.35%) and −136.15 (±0.07%). The combined-data equation covers a range of 425–575 K and at 500 K gives ΔH° and ΔS° values of 132190 J/mol and 226.10 J/(K mol), respectively. These values correlate with those from a recent pressure study, within the reported large experimental uncertainty of ±7%.[13]

Supplementary Material Available: Table IV, experimental absorbances for the samples at the various wavelengths and temperatures (3 pages). Ordering information is given on any current masthead page.

(13) Eggers, H.-H.; Ollmann, D.; Heinz, D.; Drobot, D. W.; Nikolajew, A. W. *Z. Phys. Chem. (Leipzig)* **1986**, *267*, 353-363.

Contribution from the Departments of Chemistry, Sonoma State University, Rohnert Park, California 94928, and University of Washington, Seattle, Washington 98195

Iron(III) Chloride Hydrate in the Vapor Phase

D. S. Rustad† and N. W. Gregory*,‡

Received November 10, 1987

Spectrophotometric evidence indicates that iron(III) chloride hydrate vapor molecules are of major importance in certain $FeCl_3$–Cl_2–HCl–H_2O vapor mixtures. Molar absorptivities for the hydrate vapor molecule have been derived at 10-nm intervals over the wavelength range 240–440 nm in the temperature range 415–640 K. Values for the standard enthalpy of formation, −590 kJ mol^{-1}, and the standard entropy, 471 J mol^{-1} K^{-1}, for $Fe(H_2O)Cl_3(g)$ at 500 K are derived from equilibrium data. Between 415 and 475 K, the variation of the vapor absorbance with the concentration of water vapor indicates that a condensed hydrate phase with empirical composition $Fe_2Cl_6(H_2O)_3$ is present.

Introduction

In an earlier investigation of the vapor phase generated by heating hydrogen chloride and iron(III) oxide mixtures, evidence was found for the presence of iron(III) chloride hydrate, $Fe(H_2O)Cl_3$, molecules.[1] We now report an extended spectrophotometric study of the $FeCl_3$–Cl_2–HCl–H_2O system. Vapor-phase absorbances of homogeneous mixtures with different compositions may be explained by assuming that the dominant equilibrium at temperatures below 600 K is

$$0.5Fe_2Cl_6(g) + H_2O(g) = Fe(H_2O)Cl_3(g) \qquad (1)$$

Molar absorptivities at wavelengths over the range 240–440 nm (10-nm intervals) and thermodynamic constants are derived for the gaseous hydrate molecule.

Experimental Section

The reactants (see Table I) were introduced, under vacuum, into cylindrical quartz absorption cells of 5 cm path length and 1.9 cm i.d. A quartz tube (ca. 20 cm long with 2 and 4 mm o.d. sections) was attached at the center of each cell. A small piece of iron wire (Baker and Adamson standardization wire, 99.90%) was inserted into this side arm, which was then connected to the Pyrex vacuum system by using a graded quartz–Pyrex seal. The system was evacuated. Chlorine was generated by thermal decomposition of anhydrous copper(II) chloride. The gas was liquefied, and then small amounts were vaporized (from an excess of liquid) into the cells. The mixtures were flamed lightly to form iron(III) chloride and desired amounts sublimed into the cells. Small excesses of chlorine, sufficient to prevent decomposition of iron(III) chloride into solid iron(II) chloride, and known amounts of dry hydrogen chloride (Matheson) were then condensed into the cells with use of liquid nitrogen.

Hydrogen chloride was added to prevent the interaction of water and iron(III) chloride to form iron(III) oxide and/or iron(III) oxychloride. The samples of hydrogen chloride were vaporized from an excess of condensed liquid. Amounts were calculated with use of measured pressures in calibrated volumes and the perfect-gas law. The gas passed through a dry-ice trap before it entered the cell. The mixture in each cell was then isolated by collapsing a section of the side arm.

Table I. Initial Reactant Concentrations (mol L^{-1})

sample no.	$10^6C_{FeCl_3}$[a]	$10^4C_{H_2O}$[b]	10^2C_{HCl}[b]	$10^4C_{Cl_2}$[b]
1	26.8 ± 0.5	39.7	2.56	1.0
2	9.9 ± 0.4	38.5	2.63	3.0
3	24.3 ± 0.6	(12.5)[d]	2.50	2.3
4	16.8 ± 0.3[c]	(6.90)[d]	1.02	1.0
5	8.9 ± 0.1	39.1	2.66	2.1
6	50.0 ± 1.0	15.0	2.66	2.2
7	28.1 ± 0.5	19.4	2.38	0.8
8	53.2 ± 0.9	8.59	2.58	4.4

[a] Based on an analytical determination of iron; ± values are estimated uncertainties. [b] Estimated uncertainty: H_2O, 2%; HCl, 1%; Cl_2, 5%. [c] 16.2 ± 0.3 calculated from the absorbance at 360 nm before addition of water. [d] Adjusted; see Results and Discussion.

Chlorine concentrations were determined from measured absorbances at 330 nm at room temperature; at higher temperatures the absorbances of iron(III) chloride vapors were measured at 360 nm to see that the desired amounts were present.[2] The calculated spectral concentrations of iron agreed with those found by analysis except for sample 4 (see Table I). Absorbances were measured with a Cary 14H spectrophotometer.

The cells were then reconnected to the vacuum system and measured amounts of water introduced by one of two methods. For three samples a short piece of thick-walled Tygon tubing was used. The side arm of a sealed cell was scored with a file and slipped into the snug-fitting tubing that was connected to the vacuum system. After evacuation of the assembly, the tip was broken off by bending the tubing and then a measured amount of water vapor was condensed into the cell, cooled with liquid nitrogen.

In the second method, used for the other samples, a slightly larger section (4 mm o.d.) of the quartz side arm of a sealed cell was slipped into a tight-fitting tubular end of a Pyrex ball joint and sealed with black vacuum wax. The tip of the side arm (2 mm o.d.), scored with a file near the ball joint, extended through the joint into the matching half that was attached to the vacuum system. After evacuation of the assembly, the tip was broken off by tilting the halves of the joint slightly. A measured quantity of water vapor was then condensed into the cell, cooled with liquid nitrogen.

† Sonoma State University.
‡ University of Washington.

(1) Gregory, N. W. *Inorg. Chem.* **1983**, *22*, 3750-3754.
(2) Rustad, D. S.; Gregory, N. W. *Inorg. Chem.*, preceding paper in this issue.

0020-1669/88/1327-2840$01.50/0

Quantities of water were measured in one of two ways. Before transfer to the cell (a) a sample of water vapor was isolated in a known volume at ca. 24 °C and its pressure (range 8–14 Torr) was measured or (b) water vapor at the triple-point pressure (4.58 Torr), established by equilibration with an ice–liquid water mixture, was collected in a known volume at room temperature. In both cases the number of moles of water was calculated by assuming the ideal-gas law.

After introduction of the water the quartz side arms were sealed again, the cells heated, and the spectra recorded. The apparatus (furnace) designed to heat the cells has been described previously.[1,3]

Temperatures at the middle of the cell body (T_1), the edges of the cell windows (T_2), and the tip of the side arm (T_3) were measured with chromel–alumel thermocouples, calibrated at the boiling point of water and the melting point of tin. T_1 and T_2 were controlled together and independently of T_3 by using separate heating elements. T_1 and T_3 were kept the same when samples were fully vaporized. When a condensed phase was present, T_3 was kept several degrees colder than T_2 to keep the condensate in the tip at T_3. The maximum difference between T_1 and T_2 was 6 K. T_1 was taken as the temperature of the gas mixture.

After completion of the absorbance measurements, the amounts of iron in the cells were determined by analysis with ICP emission spectrometry (Model 955 Plasmo Atomcomp).

Results and Discussion

Completely vaporized mixtures (Table I) were studied between 475 and 640 K, and vapor mixtures with a condensed hydrate phase present, between 415 and 475 K. At the higher temperatures, the equilibrium between monomeric and dimeric iron(III) chloride

$$2FeCl_3(g) = Fe_2Cl_6(g) \quad (2)$$

must be considered along with equilibrium 1. The contributions of chlorine and hydrogen chloride—HCl does not absorb significantly in the wavelength range studied—were subtracted from the total absorbance. The remainder was divided by the cell path length to derive values of A_λ, the absorbance at a particular wavelength λ. On the basis of findings of the previous study,[1] we initially assumed that A_λ was determined by the contributions of the hydrate (H), dimer (D), and monomer (M):

$$A_\lambda = \epsilon_{\lambda,H}C_H + \epsilon_{\lambda,D}C_D + \epsilon_{\lambda,M}C_M \quad (3)$$

In eq 3, ϵ_λ represents the molar absorptivity and C represents the concentration of the various species identified by the associated subscript.

Absorbances of Completely Vaporized Mixtures at 360 nm. A maximum is observed in the absorption spectrum of $Fe_2Cl_6(g)$ (D) at 360 nm.[2] The earlier evidence[1] for the presence of $Fe(H_2O)Cl_3(g)$ (H) was also based on absorbance data measured at 360 nm. Hence, in the present work, the validity of eq 3 and the associated assumption that the concentrations C_D, C_H, and C_M are related by equilibrium constants for reactions 1 and 2 were first tested with absorbance data measured at 360 nm. For reaction 1

$$K_P = \frac{P_H}{P_{H_2O}(P_D)^{1/2}} = \frac{C_H}{C_{H_2O}(C_D RT)^{1/2}}$$

We define K_1, the corresponding spectrophotometric equilibrium constant, as

$$K_1 = \frac{\epsilon_{\lambda,H}C_H}{C_{H_2O}(\epsilon_{\lambda,D}C_D RT_1)^{1/2}} \quad (4)$$

Similarly, for reaction 2

$$K_2 = \frac{\epsilon_{\lambda,D}C_D}{(\epsilon_{\lambda,M}C_M)^2 RT_1} \quad (5)$$

At 360 nm, eq 3 becomes

$$A_{360} = C_{H_2O}K_1(\epsilon_{360,D}C_D RT_1)^{1/2} + \epsilon_{360,D}C_D + \left(\frac{\epsilon_{360,D}C_D}{K_2 RT_1}\right)^{1/2} \quad (6)$$

K_2 values were derived from molar absorptivities[2] and thermodynamic data[4] for Fe_2Cl_6 and $FeCl_3$. K_1 was initially taken as $\exp((2610/T_1) - 2.176)$, derived from the study of the Fe_2O_3–HCl system.[1] Equation 6 was then solved for $\epsilon_{360,D}C_D$, and subsequently $\epsilon_{360,M}C_M$ and $\epsilon_{360,H}C_H$, without knowledge of the molar absorptivity of the hydrate, $\epsilon_{360,H}$.

The experimental uncertainty of the result derived for K_1 in the HCl–Fe_2O_3 study[1] is very large. The least-squares standard deviation for the enthalpy constant was 10% and for the entropy–molar absorptivity constant 24%. In that work the heterogeneous mixtures approached equilibrium very slowly, photolysis effects were troublesome, and an appreciable temperature gradient was necessary to prevent deposition of solids on the cell windows. The concentration of water vapor was necessarily based on the equilibrium constant[5,6] for reaction 7 and the initial pressure of

$$Fe_2O_3(s) + 2HCl(g) = 2FeOCl(s) + H_2O(g) \quad (7)$$

HCl. For the mixtures studied in the present work these problems were largely eliminated. Cell temperatures were kept uniform for fully vaporized samples, and generally chemical equilibrium was reached by the time the system was in thermal equilibrium. The high concentration of hydrogen chloride eliminated photolysis problems, probably by decreasing the rate of condensation of iron(II) chloride. Since the amount of water tied up in the hydrate molecules was generally much less than 1% (maximum, in only a few cases, 1.4%) of the total amount present, the concentration of water vapor was fixed by the amount introduced into the cell.

With data measured in the present study, the equation $K_1 = \exp((2610/T_1) - 2.12)$, i.e. a slightly lower entropy constant, gave a better overall fit between observed and calculated absorbances. Results from samples 3 and 4 were not compatible with the others until the concentrations of water vapor were increased (ca. 15%) to the values shown in parentheses in Table I. In these cases the water samples were transferred to the cells with use of Tygon tubing (see Experimental Section). It is concluded that some additional water was desorbed from the Tygon during the transfer. In a subsequent experiment a measurable amount of water was trapped over long periods of pumping on a comparable section of the Tygon tubing. Sample 5, prepared with use of Tygon tubing, did not show anomalous behavior. The second method used to open sealed cells is recommended as a more satisfactory procedure. Values of $\epsilon_{360,D}C_D$, $\epsilon_{360,M}C_M$, and $\epsilon_{360,H}C_H$, derived for each of the 59 observations (from 8 independent samples) are listed in Table II.

Absorbances at Other Wavelengths. At other selected wavelengths eq 3 was written

$$A_\lambda = R_{\lambda,H}(\epsilon_{360,H}C_H) + R_{\lambda,D}(\epsilon_{360,D}C_D) + R_{\lambda,M}(\epsilon_{360,M}C_M) \quad (8)$$

where the R_λ term for each component represents a molar absorptivity ratio, e.g. $R_{\lambda,H} = \epsilon_{\lambda,H}/\epsilon_{360,H}$. Empirical equations expressing $R_{\lambda,D}$ and $R_{\lambda,M}$ as linear functions of temperature, fitted in the same temperature range, were taken from ref 2. In that study the uncertainties in the data did not justify inclusion of higher powers of the temperature or use of a more complex relationship. With these R values and values of $\epsilon_{360,H}C_H$, $\epsilon_{360,D}C_D$, and $\epsilon_{360,M}C_M$ (from Table II), eq 8 was used to derive a value of $R_{\lambda,H}$ for each measured value of A_λ. The temperature dependence of $R_{\lambda,H}$ at each wavelength was also approximated by a least-squares fit to the empirical linear form $R_{\lambda,H} = a + bT_1$ (see Table III).

Values of $R_{\lambda,H}$ at each wavelength (Table III) were calculated at 450, 500, 550, and 600 K and integrated areas derived (with use of Simpson's one-third rule) for the range 240–440 nm at each temperature. Assuming vibronic spectra, an integrated area for

(3) Hilden, D. L. Ph.D. Thesis, University of Washington, Seattle, WA, 1971.

(4) Chase, M. W., Jr.; Davies, C. A.; Downey, J. R., Jr.; Frurip, D. J.; McDonald, R. A.; Syverud, A. N. *JANAF Thermochemical Tables*, 3rd ed.; American Chemical Society and American Institute of Physics: New York, 1986.

(5) Gregory, N. W. *Inorg. Chem.* **1983**, *22*, 2677–2680.

(6) Stuve, J. M.; Ferrante, M. J.; Richardson, D. W.; Brown, R. R. *Rep. Invest.—U.S. Bur. Mines* **1980**, *No. RI-8420*.

Table II. Vapor Absorbances at 360 nm, A_{360}, and 340 nm, A_{340}, for Various Samples and Calculated Contributions from Hydrate, Dimer, and Monomer[a]

sample no.	T_1, K	T_3, K	λ_{max}, nm	$10A_{360}$	$10A_{340}$	$10\epsilon_{360,H}C_H$	$10\epsilon_{360D}C_D$	$10\epsilon_{360,M}C_M$	DIF, %	X_H, %	10^6C_{Fe}(calcd)
1	538.4	538.4	343	1.566	1.654	0.971	0.584	0.012	−1.3	61	27.3
1	586.0	586.0	345	1.556	1.580	0.770	0.739	0.047	1.0	49	27.6
1	623.7	623.7	347	1.506	1.502	0.620	0.772	0.113	2.4	41	26.9
2	493.0	493.0	340	0.462	0.566	0.412	0.050	0.001	−0.5	89	8.0
2	532.0	532.0	340	0.478	0.550	0.386	0.088	0.004	−2.1	80	8.4
2	577.0	577.0	340	0.478	0.526	0.333	0.129	0.016	−1.0	69	8.5
2	630.2	630.2	340	0.468	0.496	0.258	0.152	0.058	0.7	55	8.3
3	476.7	476.7	350	1.416	1.384	0.624	0.790	0.002	0.7	44	23.8
3	534.2	534.2	354	1.420	1.260	0.412	0.994	0.014	−0.2	29	24.4
3	577.7	577.7	356	1.396	1.194	0.305	1.046	0.045	−0.8	21	24.4
3	633.4	633.4	358	1.368	1.168	0.210	1.000	0.158	−0.6	15	24.3
3	427.4	415.0		0.070	0.090	0.067	0.003	0.000	−0.7	95	
3	436.2	425.4	340	0.184	0.226	0.163	0.021	0.000	−1.4	88	
3	448.7	435.7	344	0.386	0.448	0.293	0.093	0.000	−0.4	75	
3	457.7	445.2	348	0.882	0.938	0.520	0.362	0.001	0.3	58	
3	462.2	448.0	348	1.114	1.136	0.592	0.521	0.001	−0.6	53	
4	477.0	477.0	351	0.922	0.844	0.304	0.617	0.002	1.1	32	15.4
4	535.2	535.2	355	0.916	0.776	0.191	0.713	0.012	0.2	20	15.7
4	578.7	578.7	355	0.910	0.756	0.140	0.731	0.039	−0.1	15	15.9
4	633.2	633.2	355	0.902	0.750	0.096	0.677	0.129	−1.4	10	15.9
4	432.4	418.4		0.116	0.128	0.095	0.021	0.000	−9.2	81	
4	445.2	431.2		0.348	0.372	0.207	0.140	0.000	0.3	59	
4	453.7	443.2	350	0.880	0.844	0.360	0.520	0.001	0.8	40	
5	495.7	495.7	338	0.484	0.598	0.428	0.055	0.001	0.7	88	8.4
5	515.7	515.7	338	0.498	0.594	0.420	0.076	0.002	−0.4	84	8.7
5	530.2	530.2	339	0.492	0.580	0.400	0.089	0.004	0.1	81	8.6
5	586.2	586.2	340	0.498	0.558	0.334	0.143	0.021	2.0	67	8.9
5	641.4	641.4	340	0.498	0.528	0.256	0.166	0.076	1.8	51	8.9
5	439.0	426.4		0.066	0.092	0.066	0.000	0.000	5.9	99	
5	455.0	438.4		0.144	0.186	0.141	0.003	0.000	−0.5	98	
5	466.0	451.4	336	0.398	0.508	0.375	0.023	0.000	0.5	94	
6	447.2	442.2	340	0.590	0.676	0.446	0.144	0.000	−1.5	75	
6	462.2	448.2	345	0.934	1.002	0.584	0.350	0.001	−0.8	62	
6	464.2	455.4	348	1.584	1.628	0.833	0.75	0.001	0.6	52	
6	472.0	460.7	350	2.446	2.368	1.043	1.401	0.002	0.6	42	
6	473.7	473.7	351	2.948	2.812	1.157	1.789	0.002	1.2	39	49.4
6	503.4	503.4	353	2.964	2.670	0.921	2.035	0.007	0.5	31	50.2
6	522.7	522.7	355	2.942	2.578	0.795	2.133	0.014	0.1	27	50.3
6	553.0	553.0	357	2.902	2.484	0.637	2.230	0.035	0.3	21	50.3
6	582.0	582.0	358	2.852	2.408	0.521	2.257	0.074	0.2	18	50.0
7	439.7	430.2	338	0.142	0.190	0.135	0.007	0.000	3.9	95	
7	464.4	442.2	340	0.394	0.474	0.326	0.068	0.000	0.1	82	
7	472.4	455.4	346	1.106	1.192	0.714	0.391	0.001	−1.3	64	
7	473.2	473.2	349	1.656	1.720	0.949	0.705	0.001	−1.0	57	28.0
7	497.2	497.2	350	1.680	1.648	0.822	0.854	0.004	−1.8	48	28.6
7	543.7	543.7	354	1.656	1.528	0.604	1.033	0.018	−0.9	36	28.7
7	588.7	588.7	356	1.624	1.444	0.452	1.110	0.061	−0.8	27	28.6
7	623.7	623.7	356	1.606	1.416	0.363	1.108	0.136	−0.4	22	28.5
8	441.4	433.4	348	0.424	0.472	0.277	0.147	0.000	1.1	65	
8	450.7	438.2	348	0.666	0.682	0.358	0.308	0.000	−0.5	53	
8	457.2	448.0	352	1.510	1.406	0.575	0.934	0.001	−0.4	38	
8	462.0	452.0	355	2.212	1.958	0.692	1.518	0.001	−1.0	31	
8	486.4	486.4	357	3.148	2.646	0.682	2.462	0.004	0.1	21	52.6
8	514.7	514.7	357	3.084	2.544	0.532	2.540	0.012	0.6	17	52.3
8	543.2	543.2	359	3.050	2.480	0.424	2.597	0.028	0.7	13	52.4
8	574.0	574.0	359	3.004	2.440	0.338	2.601	0.065	1.1	11	52.4
8	464.0	450.2	352	1.714	1.572	0.585	1.128	0.001	0.6	34	
8	469.0	453.7	353	2.096	1.852	0.630	1.464	0.002	−0.5	30	
8	474.2	459.0	355	2.724	2.354	0.700	2.022	0.003	0.2	25	

Average Abs DIF = 1.1

[a] DIF = $100(A_{340}(\text{obsd}) - A_{340}(\text{calcd}))/A_{340}(\text{obsd})$. X_H is the calculated percentage of A_{360} contributed by hydrate. C_{Fe}(calcd) is the predicted amount of iron in the cell calculated from observed absorbances, derived values of K_1 and K_2, and the molar absorptivities (compare Table I).

$\epsilon_{\lambda,H}$ should be independent of temperature. Hence, the temperature dependence of the four relative areas, 12.7913 (450 K), 13.0783 (500 K), 13.3654 (550 K), and 13.6524 (600 K), was assumed to reflect the change in $\epsilon_{360,H}$ with temperature. When the temperature dependence is approximated as linear, these values give the equation

$$\epsilon_{360,H} = \epsilon_{HC}(1.0 - (3.534 \times 10^{-4})T_1)$$

When all the iron chloride in the cell is vaporized, we assume that $C_{Fe} = C_H + 2C_D + C_M$. C_{Fe} represents the concentration equivalent of the total number of moles of iron atoms in the cell. The constant ϵ_{HC} was evaluated by eq 9, applied to each sample.

$$\epsilon_{HC} = \frac{\epsilon_{360,H}C_H}{(C_{Fe} - 2C_D - C_M)(1.0 - (3.534 \times 10^{-4})T_1)} \quad (9)$$

The concentrations of dimer, C_D, and monomer, C_M, were calculated from $\epsilon_{360,D}C_D$ and $\epsilon_{360,M}C_M$ and the respective molar absorptivities. Derived values of ϵ_{HC} were very sensitive to errors in C_{Fe}; direct calculation of the molar absorptivity of the hydrate from C_{Fe} did not prove practical. The average result for each

Table III. Constants in the Equations $R_{\lambda H} = a + bT$ at Various Wavelengths λ (nm) and ϵ_{HC} (L mol^{-1} cm^{-1}) Values for Various Samples

λ	a	10^3b, K^{-1}	λ	a	10^3b, K^{-1}	λ	a	10^3b, K^{-1}	sample no.	ϵ_{HC}
240	0.213	0.484	310	0.463	0.349	380	0.075	0.863	1	7212
250	0.926	−0.083	320	0.855	0.080	390	−0.080	0.820	2	5500
260	0.945	0.211	330	1.342	−0.347	400	−0.040	0.509	3	6940
270	0.527	0.723	340	1.489	−0.396	410	0.009	0.264	4	6050
280	0.136	1.024	350	1.367	−0.291	420	0.049	0.095	5	6733
290	0.076	0.865	360	1.000	0.000	430	0.055	0.014	6	7005
300	0.175	0.661	370	0.559	0.359	440	0.064	−0.050	7	7282
									8	6347
										6920 (av)[a]

[a] With samples 2 and 4 omitted.

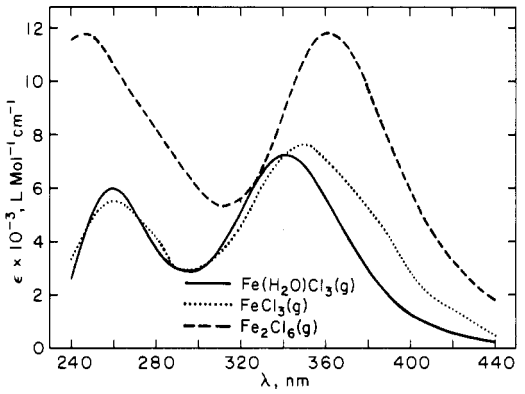

Figure 1. Absorption spectrum derived for $Fe(H_2O)Cl_3(g)$ at 523 K, based on the best fit for $R_{\lambda,H}$ Values (Table II) and $\epsilon_{360,H} = 5640$ M^{-1} cm^{-1} (see Results and Discussion). Spectra for $Fe_2Cl_6(g)$ and $FeCl_3(g)$ are shown for comparison.

sample is listed in Table III. Samples 2 and 4 deviate appreciably from the others and were omitted in the calculation of an overall average. For our temperature range we propose the equation $\epsilon_{360,H} = 6920 - 2.45T$ for the molar absorptivity of $Fe(H_2O)Cl_3(g)$ at 360 nm. The uncertainty is indicated by the range shown in Table III. These values, together with $R_{\lambda,H}$ from Table III, lead to the absorption spectrum for the hydrate shown in Figure 1; spectra for Fe_2Cl_6 and $FeCl_3$ are shown for comparison.

The ultraviolet and visible spectra of iron(III) chloride in several anhydrous alkyl and cyclic ethers at room temperature have been reported.[7] The two of the three λ_{max} values that occur in the wavelength range of the present work range from 340 to 342 and 250 to 272 nm with molar absorptivities of 5880–8825 and 4809–8615 L mol^{-1} cm^{-1}, respectively. The λ_{max} values and molar absorptivities found for the hydrate in this study are quite similar.

The overall consistency of the absorbances with the assumption that only three absorbing species are present and with the assumed equation for K_1 was tested further by using the equation

$$R_{\lambda,H}A_{360} - A_\lambda = (R_{\lambda,H} - R_{\lambda,D})\epsilon_{360,D}C_D + (R_{\lambda,H} - R_{\lambda,M})\epsilon_{360,M}C_M \quad (10)$$

$R_{\lambda,H}$ values were now taken from Table III and $R_{\lambda,D}$ and $R_{\lambda,M}$ values from previously reported absorptivities.[2] A_{360} and A_λ are the observed absorbances. With $\epsilon_{360,M}C_M$ set equal to $(\epsilon_{360,D}C_D/K_2RT)^{1/2}$, K_2 being defined above, eq 10 may be solved for $\epsilon_{360,D}C_D$, $\epsilon_{360,M}C_M$, and subsequently, with use of A_{360}, for $\epsilon_{360,H}C_H$ and a value of K_1 for each value of A_λ. A least-squares treatment of 192 observations, those with $\epsilon_{360,D}C_D$ less than 0.005 and/or with $\epsilon_{360,H}C_H$ less than 0.01 and/or with abs$(R_{\lambda,H} - R_{\lambda,D})$ less than 0.30 excluded because of the relatively larger effect of uncertainties in these cases, gave $K_1 = \exp((2603/T_1) - 2.12)$ with standard deviations in the two constants of 3.0% and 7.0%, respectively. The constants are virtually the same as those initially used but have substantially improved standard deviations as compared with those from the HCl–Fe_2O_3 study. As an example of the fit, differences between observed and calculated values of A_{340} are listed in Table II, along with the original calculated contribution of each component to the absorbance at 360 nm. However, a test of the effect of changing the enthalpy and entropy–molar absorptivity constants showed that nearly as good a fit could be achieved with other values in this range. Estimated uncertainties are 2603 (±300) and 2.12 (±0.5); the uncertainties must be applied cooperatively so as to give similar values of K_1.

Data were also tested by an evolving factor analysis treatment[8] that showed only two (dimer and hydrate) or three (dimer, hydrate, and monomer) absorbing components, depending on the temperature of the various samples. With use of absorbances for 18–22 wavelengths per sample, the samples were combined in various orders such as increasing water or iron concentrations at a given temperature. Samples with no added water were taken from a parallel study.[2]

In the vicinity of 350 nm, the wavelength at which the total absorbance is a maximum, λ_{max} (Table II), correlates with the calculated fraction of the absorbance contributed by the hydrate, X_H. When X_H is small, λ_{max} is near 360 nm, the value observed for Fe_2Cl_6; as X_H increases, λ_{max} moves toward shorter wavelengths. The maximum for the hydrate appears to be in the range 336–340 nm (also see Figure 1). A similar behavior was observed in the earlier study.[1]

The percentage difference between A_{340}(obsd) and A_{340}(calcd), DIF (Table II), is, in nearly all cases, well within experimental uncertainty. We estimate the combined uncertainty of the four absorbance measurements, two base lines and two observations, to be in the range 0.002–0.003. An error in the concentration of water will have a systematic effect (DIF tending to be too large or too small) for each sample. Uncertainties in the molar absorptivities of monomer and dimer cause an uncertainty of about 1% in the calculated absorbances at 360 nm. Some uncertainty is also associated with the temperature.

Values of $R_{\lambda,H}$ (Table III) were used together with $R_{\lambda,D}$ and $R_{\lambda,M}$ to calculate the expected absorbance and A_λ(obsd) − A_λ(calcd) value for each of the 686 observations. The average difference for all wavelengths was 2.4%. This good overall fit supports our initial assumptions. A complete list of the observed absorbances is available as supplementary material (Table IV).

With $\epsilon_{360,H}$ taken as $6920 - 2.45T$ and $\epsilon_{360,D} = 15\,504 - 7.03T$, thermodynamic equilibrium constants for reaction 1

$$K = \frac{P_{Fe(H_2O)Cl_3}}{P_{H_2O}(P_{Fe_2Cl_6})^{1/2}}$$

were calculated from K_1. A least-squares treatment gave the equation $K = \exp((2564/T) - 5.99)$. Corresponding enthalpy and entropy values are $\Delta H° = -21.3$ (3.0%) kJ mol^{-1} and $\Delta S° = -49.8$ (2.5%) J mol^{-1} K^{-1} (standard deviations in parentheses). For $Fe_2Cl_6(g)$ $\Delta H° = -650.9$ kJ mol^{-1} and $S° = 628.5$ J mol^{-1} K^{-1} at 500 K.[4] These, together with values[4] for $H_2O(g)$, lead to a standard enthalpy of formation and a standard entropy for $Fe(H_2O)Cl_3$ at 500 K of −590.4 kJ mol^{-1} and 471.2 J mol^{-1} K^{-1}, respectively.

(7) McCusker, P. A.; Kennard, S. M. S. *J. Am. Chem. Soc.* **1959**, *81*, 2976–2982.

(8) Gampp, H.; Maeder, M.; Meyer, C. J.; Zuberbuhler, A. D. *Talanta* **1985**, *32*, 1133–1139.

If one assumes the bonding structure for the hydrate molecule to be

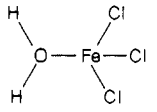

the coordinate dative Fe–O bond enthalpy (reaction 11) is found

$$Fe(H_2O)Cl_3(g) = FeCl_3(g) + H_2O(g) \qquad (11)$$

to be 93.6 kJ mol^{-1} (at 500 K). By comparison, in $FeCl_3(g)$ the average Fe–Cl bond energy is 345 kJ mol^{-1} and each bridging bond in the dimer Fe_2Cl_6 contributes 72.3 kJ mol^{-1}.[4]

Condensed Hydrate Phase. With a condensed phase present, the logarithm of the absorbance of each sample varied linearly with the reciprocal of the temperature. A "break-over" point, believed to be the temperature at which vaporization of a condensed phase was complete, was observed. At higher temperatures, the change in absorbance was assumed to be controlled by equilibria 1 and 2. When cells were removed from the furnace, a liquid phase, which often persisted at room temperature, was sometimes observed. With the liquid phase present, the vapor-phase absorbance of the various samples at a given temperature was found to depend on the concentration of water. Data for the various samples correlated well only when it was assumed that the liquid phase in each case had the empirical formula $Fe(H_2O)_{1.5}Cl_3$. $\epsilon_{360,H}C_H$, $\epsilon_{360,D}C_D$, and $\epsilon_{360,M}C_M$ values in the equilibrium vapor were derived from the total absorbance in the same way as described for the all-vapor mixtures and are included in Table II. For the proposed vaporization reaction

$$Fe(H_2O)_{1.5}Cl_3(l) = Fe(H_2O)Cl_3(g) + 0.5H_2O(g) \qquad (12)$$

the spectrophotometric equilibrium constant, K_{12}, is written

$$K_{12} = (\epsilon_{360,H}C_H RT)(C_{H_2O}RT)^{1/2}$$

Forty-two A_{360} vapor-phase absorbance values, from ten independent samples (eight in the present study, two from the $HCl-Fe_2O_3$ work[1]) were measured with the condensed hydrate phase present. With an estimated $\Delta C_P^\circ = -117$ J mol^{-1} K^{-1} for reaction 12, a least-squares treatment in the form $\Sigma = -8.314(\ln K_{12} + 14.07 \ln T_3) = \Delta H^*/T_3 + I$ gave $\Delta H^* = 152.1$ (1.9%) kJ mol^{-1} and $I = 1.047$ (0.60%) kJ mol^{-1} K^{-1}. Data are listed in Table V (supplementary material). With $\epsilon_{360,H}$ taken as $6920 - 2.45T$, the standard Gibbs free energy change for reaction 12 becomes $\Delta G^\circ = 152\,846 + 117T \ln T - 976.2T$ J mol^{-1}. At the mean temperature of 456 K, $\Delta H^\circ = 99.4$ (1.9%) kJ mol^{-1} and $\Delta S^\circ = 141.5$(0.64%) J mol^{-1} K^{-1} (standard deviations in parentheses).

The results for all samples are shown in Figure 2 and closely approximate the linear behavior expected for a Σ vs $1/T_3$ plot. Hence, within the experimental uncertainty, the composition of the liquid phase does not appear to differ significantly in the various samples. The mixtures included in Figure 2 are quite different. In those generated by the $HCl-Fe_2O_3$ reaction, the hydrate phase is presumed to be in equilibrium with Fe_2O_3(s) and FeOCl(s). The overall C_{Fe}/C_{H_2O} ratios for the eight samples of the present work differ by as much as 30, ranging from 2×10^{-3} to 6×10^{-2}.

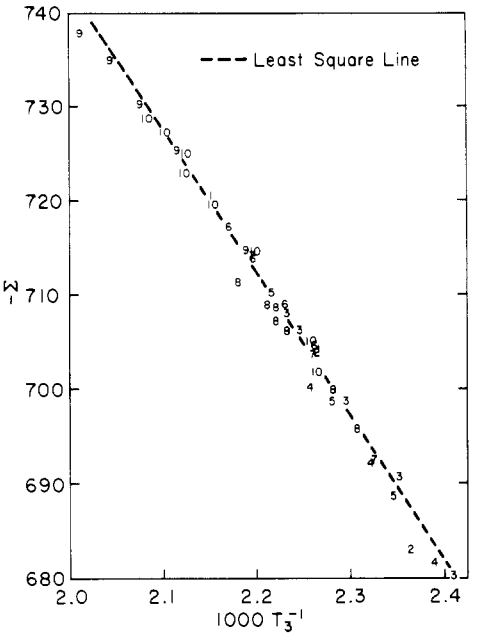

Figure 2. Σ plot. The numbers shown identify the sample (see Table I). Samples 9 and 10 are from the $HCl-Fe_2O_3$ study.[1]

The empirical composition $Fe(H_2O)_{1.5}Cl_3$ corresponds to $Fe_2Cl_6(H_2O)_3$ or, alternatively, $Fe(H_2O)_6^{3+} + 3FeCl_4^-$. Asakura, Nomura, and Kuroda[9] conclude, from X-ray absorption spectra, that in 0.1–1 M solutions of $FeCl_3$ the $Fe(H_2O)_6^{3+}$ ion, along with $FeCl(H_2O)_5^{2+}$, is of major importance and, as the $FeCl_3$ concentration increases to 3–4 M, $FeCl_2(H_2O)_4^+$ becomes dominant. At the higher temperatures of our measurements, 415–475 K, it does not appear, from the correlation based on reaction 12, that our condensates should be considered aqueous solutions. Magini[10] examined the highly concentrated melt $FeCl_3(H_2O)_6$ by X-ray diffraction and concluded that polynuclear species were present along with ionic species and that the dimer, Fe_2Cl_6, was the most probable polynuclear species.

The overall treatment of both the all-vapor and condensed-phase data was repeated in a parallel calculation with the assumption that the hydrate vapor molecule was $Fe_2(H_2O)Cl_6$. The fit between calculated and observed absorbances on this basis was unsatisfactory. While minor amounts of dimer hydrate may be in the vapor, we find no evidence to prove its presence.

Supplementary Material Available: Table IV, absorbance data at 10-nm intervals over the range 240–440 nm, and Table V, data used to construct Figure 2 (3 pages). Ordering information is given on any current masthead page.

(9) Asakura, K.; Nomura, M.; Kuroda, H. *Bull. Chem. Soc. Jpn.* **1985**, *58*, 1543–1549.
(10) Magini, M. *J. Chem. Phys.* **1982**, *76*, 1111–1115.